Control of the capillary instability process during hydrodynamic impact on the reservoir

Geylani M. Panahov · Eldar M. Abbasov · Gulshan R. Agayeva · Ibrahim J. Mamedov

Abstract. *Heterogeneous flows and immiscible fluid displacement in porous media are key topics in oil reservoir filtration studies. These processes are critical for reducing hard-to-recover oil and optimizing tertiary oil recovery methods. The complex pore structure significantly influences hydrodynamics and fluid distribution. Reservoir stimulation using physico-chemical and hydrodynamic methods significantly enhances oil recovery. Managing hydrodynamic conditions at the displacement front is crucial for mobilizing trapped oil, overcoming capillary pressure, and optimizing reservoir performance. Laboratory studies highlight capillary processes and displacement front instability as key factors influencing residual oil saturation. Optimizing reservoir impact through periodically increasing hydrodynamic pressure can improve oil recovery outcomes.*

Keywords. Heterogeneous flows · immiscible fluid displacement · porous media · oil reservoir · capillary number · reservoir stimulation · hydrodynamic pressure optimization.

Mathematics Subject Classification (2010): 76N25

Panahov G.M.
Institute of Mathematics and Mechanics of Science and Education
Ministry Republic of Azerbaijan, Baku, Azerbaijan Baku, Azerbaijan
E-mail: pan_vniineft@rambler.ru

Abbasov E.M.
Institute of Mathematics and Mechanics of Science and Education
Ministry Republic of Azerbaijan, Baku, Azerbaijan Baku, Azerbaijan
emaileldarab@gmail.com

Agayeva G.R.
Institute of Mathematics and Mechanics of Science and Education
Ministry Republic of Azerbaijan, Baku, Azerbaijan Baku, Azerbaijan
emailagayevagulshan@yahoo.com

Mamedov I.J.
Institute of Mathematics and Mechanics of Science and Education
Ministry Republic of Azerbaijan, Baku, Azerbaijan Baku, Azerbaijan
emailimamedoff1997@list.ru

1 Introduction

Heterogeneous flows, processes of immiscible fluid displacement in porous media, and the mechanisms of observed effects are the subject of numerous studies on filtration in oil-saturated reservoirs. The keen interest in such processes is driven by the search for ways to reduce the share of hard-to-recover oil in the total balance of produced hydrocarbons. Methods and technologies for extracting residual reserves are the primary objective of tertiary oil recovery methods. In all the aforementioned processes, the research object is the complex structure of the pore space, which significantly influences the hydrodynamics and distribution of saturating fluids.

Researchers in their studies [28, 21, 32] have noted that the key parameters affecting the displacement front structure are the viscosity ratio of the displaced and displacing fluids $M = \mu_1/\mu_2$ and the capillary number N (a dimensionless similarity parameter characterizing the ratio of viscous and capillary forces) [14].

Displacement of high-viscosity oil from a reservoir by water is accompanied by instability and the formation of "fingering" effects, leading to early water breakthrough and premature water production in wells [47]. In general, considering the full range of hydrodynamic, thermal, and physical-chemical effects occurring during displacement confirms that the flow of almost any displacement agent in the reservoir can become unstable under certain conditions. For example, the displacement of high-viscosity oil in a homogeneous reservoir by a polymer solution, which is typically assumed to be a piston-like process, becomes unstable at a certain stage when polymer adsorption on the rock surfaces and several other physical-chemical processes are taken into account [19, 34, 39].

Unsteady effects may also manifest in relatively macrohomogeneous oil-saturated reservoirs. Due to high viscosity instability values (the ratio of oil to water viscosity), local breakthroughs of injected water occur, affecting the indicators of water-free and current oil recovery. In reservoirs with high residual oil saturation, significant interfaces between the oil and water phases form. This hydrodynamic situation can be utilized to implement unsteady methods of reservoir stimulation during water flooding.

For fields producing high-viscosity oil (more than 100 mPa·s), unsteady processes in the reservoir have several distinctive features. These features are determined by:

1 The significantly different response times to hydrodynamic disturbances in zones with varying permeability and fluid saturation;
2 The potential for gas evolution and degassing of oil due to pressure redistribution within the reservoir.

Alongside the positive effect of inter-reservoir flows for redirecting filtration streams toward zones with residual reserves, improper selection of well operation mode dynamics can lead to complications in field development [17, 20]. Such complications include:

1 Possible changes in the filtration-capacity properties of the near-wellbore zone;
2 The formation of an unstable displacement front in the reservoir, increasing reservoir compartmentalization with zones of high and low fluid mobility;
3 Rapid degassing of oil in interbedded layers.

One of the most effective methods for extracting high-viscosity oils is reservoir stimulation using various physico-chemical and hydrodynamic methods. These methods enable a significant increase in oil recovery factor [15, 27, 29, 31].

The challenge arises of managing the hydrodynamic situation at the displacement front by creating conditions that enhance the effect of mobilizing oil trapped in pores into the main flow, overcoming capillary pressure at a distance from the pressure source.

The manifestation of unsteady effects is possible even in relatively macrohomogeneous oil-saturated reservoirs [33]. Due to high viscosity instability values (the ratio of oil to water viscosity), local breakthroughs of injected water occur, which affect the indicators of water-free and current oil recovery. In reservoirs with high residual oil saturation, significant interfaces between the oil and water phases are formed. This hydrodynamic situation can be utilized to implement unsteady methods of reservoir stimulation during water flooding [1, 12].

For fields producing high-viscosity oil (more than 100 mPa·s), unsteady processes in the reservoir exhibit several distinctive features. These features are determined by:

1 significantly different response time to hydrodynamic disturbances in zones with varying permeability and fluid saturation;
2 potential for gas evolution and oil degassing due to pressure redistribution within the reservoir.

Alongside the positive effect of inter-reservoir flows for redirecting filtration streams toward zones with residual reserves, improper selection of the dynamics of well operation mode changes can lead to complications in field development. Such complications include:

1 possible changes in the filtration-capacity properties of the near-wellbore zone;
2 formation of an unstable displacement front in the reservoir, increasing reservoir compartmentalization with zones of high and low fluid mobility;
3 rapid degassing of oil in interbedded layers.

One of the most effective methods for extracting high-viscosity oil is reservoir stimulation using various physico-chemical and hydrodynamic methods. These methods enable a significant increase in the oil recovery factor.

The challenge arises in managing the hydrodynamic conditions at the displacement front by creating conditions that enhance the effect of mobilizing oil trapped in pores into the main flow, primarily by overcoming capillary pressure at a distance from the pressure source.

2 Capillary Effects in Porous Media

The process of oil displacement by water, especially in the case of high-viscosity oil, is inherently unstable and leads to the fragmentation of the reservoir into separate oil-saturated zones. Traditionally, the displacement process in a heterogeneous porous medium is assumed to be governed by capillary forces and the structure of the pore space. In a heterogeneous medium with a complex filtration-capacity structure, these parameters and the corresponding capillary pressure Pk' $\mathbf{P}\_k'$ differ for both phases. Depending on their sizes and pressure gradient values, numerous isolated zones with residual oil saturation are formed, where fluids may remain in an immobile, capillary-trapped state, being in dynamic equilibrium with the surrounding water filtration flow.

Studies [11, 7, 35] have shown that under capillary pressure, the displacing phase selectively occupies only capillaries and hydrophilic pores with radii greater than a critical value. At low flow velocities, pore channels saturated with oil remain immobile due to capillary forces.

This phenomenon can be described as follows: pore channels containing an immobile oil phase have sizes within the range: $r_{k_1} \leq r \leq r_{k_2} = \frac{\sigma \cos \theta}{\Delta P} = |\sigma \cos \theta k f_2 / \mu v_0|$ where r_{k_1} and r_{k_2} are the minimum and maximum radii of pores containing immobile oil, and $(\sigma \cos \theta k f_2 / \mu$ is a constant value.

From the given expression, it is evident that as the filtration velocity decreases, the size of pore channels containing immobile oil increases.

At the displacement front, breakthrough fingers emerge, forming structures of increasing complexity, similar to viscous fractals or dominant instabilities [7, 48, 46]. The degree of hydrodynamic instability of these structures is assessed using Lyapunov's method and the Hausdorff-Besicovitch dimension.

On the other hand, as the applied pressure and filtration velocity increase, a greater number of pore channels become involved in the displacement process [7, 48]. It has been established that with increasing filtration velocity, the wavelength of instability decreases [11, 7].

It should be noted that during displacement under a hydrodynamic pressure gradient, the phase distribution pattern depends on the capillary number N_c, which is evaluated as the ratio of viscous forces to capillary forces:
$N_c = \frac{\mu_2 v_2}{\sigma}$, where μ_w is the viscosity of the displacing fluid, v_w is the filtration velocity, and σ is the interfacial tension [13, 10].

The capillary number can also be expressed as $N_2 = \frac{k_0 \Delta P}{\sigma l}$ where k_0 is the permeability, ΔP is the pressure gradient, and l is the filtration length. These forms of the capillary number are not equivalent. From Darcy's law, it follows that:
$v_B = \frac{k_0}{\mu_2} f_2 \frac{\Delta P}{l}$, $v_2 \mu_2 = k_0 \mu_2 \frac{\Delta P}{l}$ or $N_1 = \frac{v_2 \mu_2}{\sigma} = \frac{k f_2 \Delta P}{\sigma l} = f_2 N_2$, where f_2 is the relative phase permeability for water, f_2 considered as a function of mobile oil saturation. Taking into account the pore space, this dimensionless complex serves as an analogue of the capillary number N_c and is defined as [13, 10]:

$$N_1' = \frac{v_2 \mu_2 l_k}{\sigma \cos \theta \sqrt{m k_0}}$$

To overcome capillary pressure at a certain distance from the well, it is necessary to generate additional "local" pressure. It is known that at a constant injection well flow rate, the filtration velocity in the reservoir will decrease with the distance RR from the well according to the law $v = Q/2\pi R m'$, where m' is the effective porosity of the reservoir. As a consequence, the "local" pressure at the displacement front will also decrease.

In heterogeneous reservoirs, the efficiency of cyclic waterflooding is higher than that of conventional waterflooding. This is due to the fact that, under waterflooding conditions, the residual oil saturation in reservoir zones with poorer reservoir properties is significantly higher than the oil saturation in the main waterflooded part of the reservoir.

As pressure increases, the elastic forces of the reservoir and fluids promote the penetration of water into zones with poorer reservoir properties, while capillary forces retain the infiltrated water during subsequent decreases in reservoir pressure. Under the influence of alternating pressure differentials, fluid redistribution occurs within the unevenly saturated reservoir, aiming to equalize saturation and eliminate capillary imbalance at the interface between oil-saturated and waterflooded zones, layers, and sections.

The emergence of alternating pressure values between layers with different saturation levels accelerates capillary countercurrent imbibition of water into oil-saturated zones (layers), facilitating water penetration from waterflooded zones into oil-saturated ones through fine pores and the migration of oil from oil-saturated zones into waterflooded ones through larger pore channels.

At low hydrodynamic pressure gradients, the advancement speed of menisci in certain pore regions is lower than the movement speed of menisci driven by capillary pressure differentials. In some of the largest pores, the hydrodynamic pressure differential is sufficient to push the trapped phase and incorporate it into the overall filtration flow. As the hydrodynamic pressure gradient increases, a growing proportion of the pores is subjected to purely hydrodynamic displacement, leading to a reduction in trapped saturation volumes.

In highly heterogeneous reservoirs, the development process ensures sufficient volumetric and areal coverage of individual sections, which enhances overall oil recovery. To

improve the coverage of zones with poor reservoir properties (immobile zones), the method of cyclic (pulsed) reservoir stimulation is widely used [6, 8, 16, 47].

However, it should be noted that the practical implementation of this method does not always yield positive results. A drawback of this type of reservoir stimulation is that during the pressure reduction phase of the injection cycle, water may not be retained in micro-heterogeneities by capillary forces [40 – 45]. As a result, the trapped oil remains in the pores and does not infiltrate into the liquid flow [49]. This has led to research aimed at developing new, more effective methods of reservoir stimulation.

This study proposes a technological solution to enhance the efficiency of oil displacement by water by creating periodically increasing hydrodynamic pressure, which allows overcoming the resistance of capillary forces throughout the injection zone. The variation in water injection pressure can be schematically represented by the following pressure variation algorithm (Fig. 1).
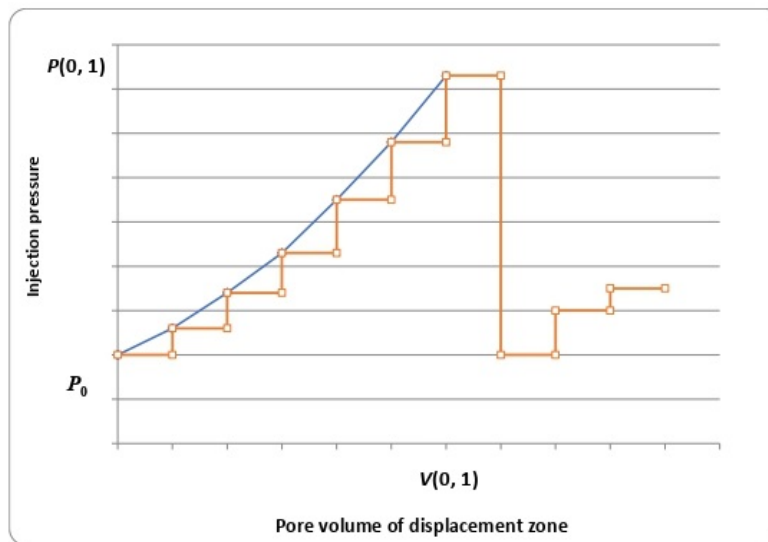

Fig. 1. Algorithm for regulating water injection pressure

When the injection rate changes, the pressure distribution rate in heterogeneous zones will vary due to differences in their reservoir properties. Consequently, oil may flow from less permeable zones to more permeable water-flooded layers, or conversely, water may flow from more permeable zones to less permeable ones. This reduces the phase permeability of the reservoir for water while increasing it for oil.

During the pressure increase phase, oil trapped in the immobile pores of the reservoir is displaced by water. Accordingly, at a distance from the well, the pore volume expands due to pressure reduction in heterogeneities where water is retained by capillary forces in the pores it has infiltrated. This process creates conditions for the release of the oil phase into the mobile zone of the reservoir.

Laboratory Studies. To confirm the proposed assumptions, laboratory experiments were conducted to simulate oil displacement conditions in a permeability-heterogeneous porous medium. Filtration experiments were carried out using the CoreTest Systems FFES 655 filtration unit for physical modeling of an oil reservoir (Fig. 2).
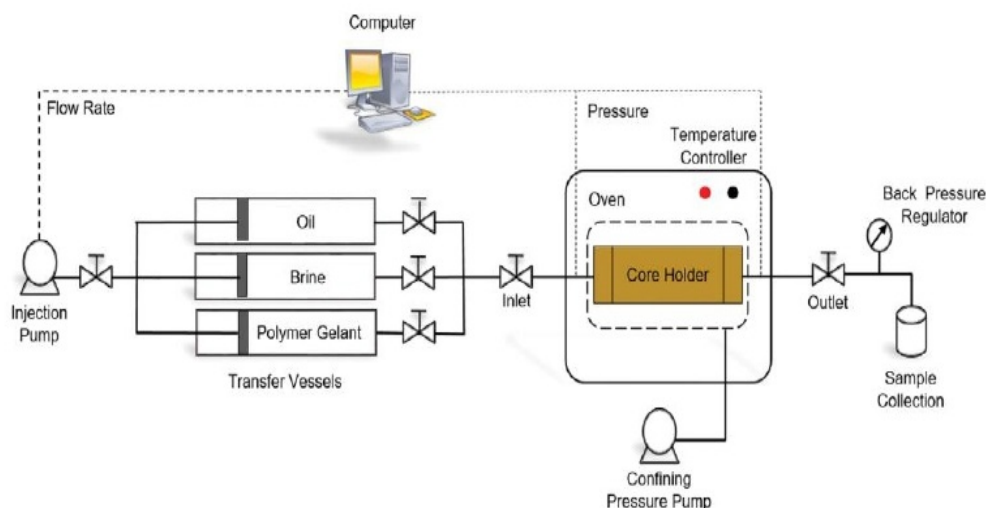
Fig. 2. Schematic diagram of the experimental setup

In the absence of water in the outgoing production, the residual water saturation was determined to be within 20%, and the oil saturation of the model was assumed to be 80%.

The displacement experiments were conducted in three stages. In the first stage, as part of the background studies, oil was displaced by water from the Bohai Bay reservoir of the CNOOC oil company (China) under a constant pressure gradient of 1.5 MPa, with an input pressure of 8.0 MPa and an output pressure of 6.5 MPa. Once the maximum displacement efficiency was achieved and the filtration process stabilized, the phase permeability of the filtration model to water was determined (Table 1).

Table 1. Physicochemical properties of the reservoir model and barodynamic parameters of oil displacement.

Temperature, $\circ^{C}$	67	Oil phase permeability at K, mD	54,3
Reservoir pressure, MPa	7	Water phase permeability at K, mD	2,2
Rock pressure, MPa	30	Water phase permeability at K after treatment, mD	1,6
Viscosity of the oil model, cP	1,68	Displacement regime, cm^3/min	0,10
Displacing agent is water, g/l	22,0	Observed GradP on the model during displacement, MPa/m	0,47
		Observed GradP on the model during displacement after treatment, MPa/m	0,62

At the second stage, under similar conditions, oil was displaced by water, causing a change in the hydrodynamic regime through a stepwise increase in injection pressure at the model's entrance. The displacement regime was determined based on the condition of displacing residual oil at increased water injection pressures. To achieve this, the pressure

at the model's entrance was stepwise increased to values $P_i = 7.06$, 7.12, and 7.18 MPa, and the pressure drop between the entrance and exit of the filtration model was recorded.

The results of the laboratory experiments are shown in Fig. 3. The dependence described shows the pressure drop dynamics during regime change: during the stage of water-free displacement, the pressure drop increases to a certain value, and with increased water cut, it decreases to 0.02 MPa. After changing the hydrodynamic regime, returning to the original displacement regime is accompanied by relatively higher values of pressure drop during the stabilization section, along with significant fluctuations in ΔP, which may indirectly indicate a change in the local hydrodynamic situation in the porous medium and the involvement of unswept pore channels and capillaries.
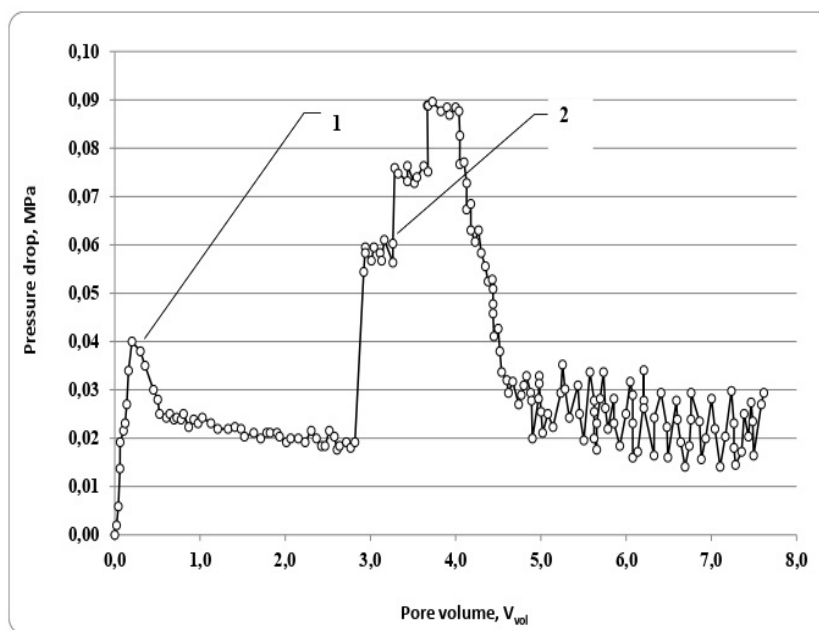
Fig. 3. Dynamics of oil displacement by a sodium carbonate solution under different hydrodynamic pressure regimes (sample permeability k_g=150 mD): 1 - displacement regime with constant injection pressure; 2 - displacement regime with increasing injection pressure

In all cases, displacement was carried out by continuous injection of solutions in the amount of 3 times the pore volume. The results of the studies presented in Figure 4 represent the dependence of oil saturation on the volume of liquid extracted from the porous medium. As seen from the figure, during oil displacement by formation water, and displacement with sequential stepped increase in injection pressure at the model entrance, the character of oil saturation change is different. The change is characterized by the fact that when oil is displaced by an aqueous solution, an additional contribution to this process is the management of the hydrodynamic situation at the displacement front by creating conditions to enhance the effect of involving the trapped oil in the pores into the overall flow, achieved by overcoming capillary pressure at a distance from the pressure source (Fig. 4, curve 3).
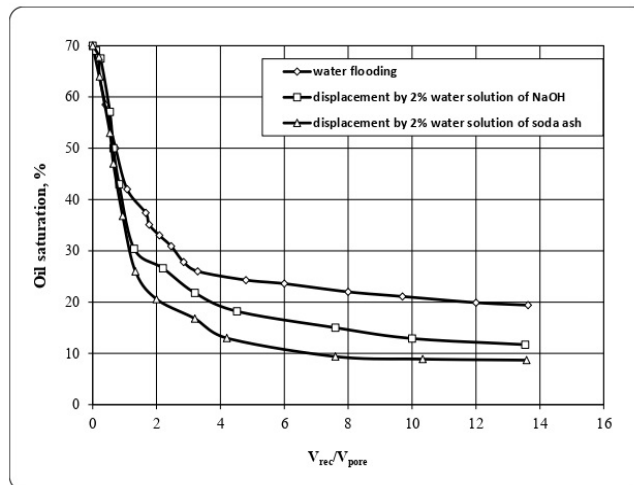
Fig. 4. Change in oil saturation of the porous medium during displacement

2. Theoretical Studies. To assess the effect of accelerating the water injection into heterogeneities using the example of a heterogeneous reservoir, let's consider the linear equation with constant coefficients:

$$\frac{du}{dt} = au + f, \qquad u(0) = e. \tag{2.1}$$

Let's perform the Laplace transform:

$$\int\limits_0^\infty e^{-st}\frac{du}{dt} = a\int\limits_0^\infty e^{-st}udt + \int\limits_0^\infty e^{-st}fdt. \tag{2.2}$$

By integrating by parts, we get:

$$e^{-st}u\Big|_0^\infty + s\int\limits_0^\infty e^{-st}udt = a\int\limits_0^\infty e^{-st}udt + \int\limits_0^\infty e^{-st}fdt\ . \tag{2.3}$$

Let's introduce a notation:

$$L(u) = \int\limits_0^\infty e^{-st}udt,\ \ L(f) = \int\limits_0^\infty e^{-st}fdt\ ,$$

let's find:

$$L(u) = \frac{c}{s-a} + \frac{L(f)}{s-a}.$$

Applying the Laplace transform and the convolution theorem, we have the equation:

$$u(t) = f(t) + \int\limits_0^t u(t-s)\,dG(s)\,, \tag{2.4}$$

where the integral is a Stieltjes integral. If $G(s)$ is a step function with discontinuities at a finite number of points $0 < t_1 < t_2 < \ldots < t_k$?, then equation (**??**) can be written as

$$u(t) = f(t) + \sum_{i=1}^{k} g_i u(t - t_i), \qquad (2.5)$$

where $u(t) = 0$ for $t < 0$.

The solution obtained by the Laplace transform:

$$u(t) = \smallint_{(G)} \frac{L(f) e^{st} ds}{1 - L(dG)}$$

can be written as

$$u(t) = \smallint_{(G)} \frac{L(f) e^{st} ds}{1 - \sum_{i=1}^{N} g_i e^{-st_i}}$$

where g_i are the jumps.

If there exists a constant $\exists c_1 = const > 0$ such that $|f(t)| \leq c_1$ on the interval $0 \leq t \leq t_0$, then there exists a unique solution to the equation. To prove this, one can use the method of successive approximations:

$$u_0(t) = f(t),$$

$$u_{n+1}(t) = f(t) + \int_0^t u_0(t - s) \varphi(s) ds.$$

Here, the condition $\int_0^{t_0} |\varphi(s)| ds < \infty$ is also needed.

There are two sub-cases. Either the numbers t_i is commensurable, or they are not. If the numbers t_i is commensurable, then for the root $S = r$, the set of roots located at equal distances from each other corresponds to $S = r \pm iktT_0$, $k = 1, 2 \ldots$ Therefore, if we assume that there is a single simple real root r, then $u(t)$ has the form:

$$u(t) = \sum_{k=-\infty}^{\infty} \frac{\left\{ \int_0^{\infty} f(t_1) exp1 - (r + ikT_0) t_i dt_i \right\} \; exp\left\{ (r + ikT_0) i \right\}}{\sum_{i=1}^{N} g_i t_i e^{-rt_i}}.$$

To justify the contour shift, we use the theorem of N. Wiener. If the numbers t_i are incommensurable, we apply the results of Bochner and Pitt.

Let us consider equation (2.1) by taking the function $P(t)$ as follows. Let it be $P(t)$ a simple discontinuous function, for example, a step function. Consider the derivative of a piecewise absolutely continuous function $P(t)$ with a piecewise continuous derivative $P'(t)$, with discontinuity points $t_1, t_2, \ldots$ and corresponding jumps $h_1, h_2, \ldots$

Let's define the function.

$$P_1(t) = P(t) - \sum_k h_k \cdot \theta(t - t_k),$$

where $\theta(t) = \begin{cases} 1, & t > 0 \\ 0, & t < 0 \end{cases}.$

It is known that $\theta'(t) = \delta$, i.e., $\theta(t)$ is zero in the usual sense for $t \neq 0$, but does not exist at $t = 0$. The function $P_1(t)$ is absolutely continuous and can be reconstructed from its derivative $P_1'(t)$. It coincides with $P'(t)$ everywhere except at the discontinuity points of $P(t)$, where $P'(t)$ does not exist. Therefore, $P_1'(t)$ is the derivative of the generalized function P_1 in the space of generalized functions.

On the other hand,

$$P_1'(t) = P'(t) - \sum_k h_k \cdot \delta(t - t_k),$$

where f' is the derivative of the generalized function $P(t)$. As a result, we obtain:

$$P'(t) = P_1'(t) + \sum_k h_k \cdot \delta(t - t_k), \tag{2.6}$$

that is, the derivative of the generalized function $P(t)$ is reconstructed from its regular derivative and the sum of delta functions at the discontinuity points with the corresponding jumps.

Next, the general solution of equation (2.1) will be in the form of:

$$\nu = \frac{1}{exp\left(\frac{\alpha t}{\mu \beta_2}\right)} \left[\frac{\alpha}{\mu} \int \left[P_1'(t) + \sum_k h_k \cdot \delta(t - t_k)\right] dt + c\right] \tag{2.7}$$

An important aspect of this process is the control of pressure distribution across the formation. The pressure redistribution after injection with a constant flow rate until the next cycle takes the form of planar radial filtration [26]:

$$\frac{\partial P}{\partial t} = \chi \left(\frac{\partial^2 P}{\partial r^2} + \frac{1}{r} \frac{\partial P}{\partial r}\right) \tag{2.8}$$

with initial and boundary conditions:

$$P(r, t) = P_{k_i} = Const \; ; at \; t = 0$$

$$Q_1 = \frac{2\pi kh}{\mu}\left(r_1 \frac{\partial P}{\partial r}\right)_{r=r_1} \qquad Q_1 = 0 \text{ at } r = 0; \tag{2.9}$$

$$P(r, \, t) = \left(P_{k_i} - \frac{Q\mu r}{\omega k}\right)_{r=r_1}$$

where Q_1 is the fluid flow rate, tt is time, and χ is the piezoconductivity.

The exact solution has the following form [49, 26]:

$$P_{k_i} - P(r, t) = \frac{Q\mu}{4\pi kh} E_i\left(-\frac{r^2}{4\chi t}\right), \tag{2.10}$$

where P_{k_i} is the injection pressure. As shown in [26, 24], for small values of

$$E_i\left(-\frac{r^2}{4\chi t}\right) = \int\limits_{\frac{r^2}{4\chi t}}^{\infty} \frac{l^4}{u} du = \ln \frac{4\chi t}{r^2} - 0,5772,$$

from (2.10), we will obtain:

$$P_{k_i} - P(r, t) = \frac{Q\mu}{4\pi kh}\left(\ln \frac{4\chi t}{r^2} - 0,5772\right) \tag{2.11}$$

The pressure at any point in the formation at any time during the injection process of elastic fluid parallel to the X-axis at constant pressure $(P_{ki} - P_{k(i-1)})$ and filtering under unsteady conditions can be obtained by integrating the equation:

$$\frac{\partial P}{\partial t} = \chi \frac{\partial^2 P}{\partial x^2} \qquad (2.12)$$

with the initial and boundary conditions:

$$P(x,0) = 0 \text{ for } t = 0 \quad P(0,t) = P_{k_i} \text{ for } x = 0 \qquad (2.13)$$

$$v(0,\ t) = Const; \ P(x,\ t) = \left(P_{ki} - \sqrt{\tfrac{3}{2}} \tfrac{\mu \sqrt{\chi t}}{k} v\right), \quad \text{for} \quad x = \infty.$$

Due to the complexity of obtaining exact solutions and to ensure the accessibility of parameter estimation for the equation, various methods for solving unsteady-state filtration problems for elastic fluid are proposed. One of the most common approximate methods is the method of sequential change of stationary states [24]. If the fluid flow rate does not change over time at each stage of the injection, i.e.,

$$Q(0,\ t) = Const,$$

$$P(x,t) = P_{k_i} - (P_{k_i} - P)\frac{x}{l(t_i)}$$

where:

P_{k_1} – injection pressure; P – pressure at the contour of movement.

As is known [24], the distribution of the front is:

$$\Delta P = (P_{k_i} - P) = \sqrt{\frac{3}{2}} \frac{\mu}{k} v \sqrt{\chi t} \qquad (2.14)$$

Under the condition $P > P'_k$, there is possible fluid exchange between the immobile and mobile parts of the formation, where $P'_k = \frac{2\sigma \cos \theta}{r}$.

Conditions provided at the radius of the contour $P \leq P'_k$ imply that the injection pressure must be increased again.

The time for pressure propagation is estimated as:

$$t = \left[\frac{(P_{k_i} - P)k}{\mu \chi \sqrt{\frac{3}{2}}}\right]^2. \qquad (2.15)$$

Given the known formation parameters, the influence radius can be determined. Described influence radius is derived from the material balance equation and known from t (2.10) [24]:

$$l(t) = \sqrt{6\chi t} = \sqrt{6\chi} \frac{\left(P_{k_i} - P_{k(i-1)}\right) k}{\mu \chi \sqrt{3/2}} \qquad (2.16)$$

where $\chi = \frac{kK}{\mu m}$; $K = \frac{m}{\beta^*}$, where $\beta^* = m\beta_6 + \beta$ is the compressibility coefficient of the fluid and porous medium. Using equations (2.8), (2.9), (2.10), and (2.7), the value of $P(x, t)$ can be estimated.

The fluid exchange between the mobile and immobile zones occurs due to the increased average pressure differential between them.

The task described is technologically implemented through the following stages:

1 at time $t = 0$, the pressure in the injection gallery is instantly increased from P_0 to P_1 and maintained constant for some period t_1. The operating gallery continues to function at its previous mode;

2 at time $t=t_1$, the injection of water into the injection well continues, thereby instantly raising the pressure at its bottomhole to $P=P_2$;

3 second stage continues for some time t_2, after which the 1st and 2nd stages, etc., repeat for each (k_i), i=1, 2,..., n(k_i), i = 1, 2, ... n;

4 at the last stage of influence (k_n), at the end of the time interval t_i, the pressure drops back to its initial (formation) level P_0;

5 above stages are repeated.

It is also necessary to define the operational parameters required for field implementation of the technological solution:

a) The distribution of increased pressure at any point in the immobile and mobile zones of the formation at any time during all stages of pressure regulation; b) the duration of the injection stage; c) the average capillary pressure P_k'.

With known formation parameters, the conditions (a), (b), and (c) can be estimated as follows. The "replacement" pressure or the radius of the next stage of influence on the formation pressure due to countercurrent capillary imbibition is determined by the following geological-physical characteristics of the formation [24]:

k = 400 mD, m = 0,15; $\sigma = 35 \cdot 10^{-6}$ kg/cm^2 = $34,4 \cdot 10^{-3}$ N/m; $\cos\theta = 0,6$;

$\mu = 1,2 \cdot 10^{-3}$ Pa·s; $\beta_A = 0,306 \cdot 10^{-10}$ m^2/N; $\beta_6 = 4,59 \cdot 10^{-10}$ m^2/N;

$P_i - 20$ ÌPà; t = 3 day.

Q = 100 m^3/day;

B = 250 m;

h = 10 m.

$$l(t) = \sqrt{6\chi t};$$

t = 3 day = 3 ·0,864 ·10^5=2,6 ·10^5 s;

$$\chi = \frac{k}{\mu(m\beta_6 + \beta_A)} = \frac{0,4 \cdot 1,02 \cdot 10^{-12}}{1,2 \cdot 10^{-3}(0,15 \cdot 4,59 \cdot 10^{-10} + 0,306 \cdot 10^{-10})} = 3,42\ m^2/s;$$

$l(t) = 2,3 \cdot 10^3$ m.

$$P(x,\ t) = 20 - (20 - P)\left(\frac{x}{l(t)}\right)$$

$$(20 - P) = \sqrt{\frac{3}{2}\frac{1,2 \cdot 10^{-3}}{0,4 \cdot 1,02 \cdot 10^{-12}}} \cdot 9,4 \cdot 10^2 \cdot v$$

$$v = \frac{100}{250 \cdot 10} = 0,04\frac{m}{day} = 4,6 \cdot 10^{-7}\frac{m}{s};$$

$$(20 - P)\,1,225 \cdot \frac{1,2 \cdot 10^{-3} \cdot 9,4 \cdot 10^2 \cdot 4,6 \cdot 10^{-7}}{0,4 \cdot 1,02 \cdot 10^{-12}} = \frac{1,2 \cdot 10^2 \cdot 9,4 \cdot 10^2 \cdot 4,6}{0,4 \cdot 1,02} \cdot 1,225 =$$
$$= 156 \cdot 10^4 = 1,6$$

$$P(x,t) = 20 - (20 - P)\frac{x}{l(t)}$$

$$P(x,t) = 20 - 1,6 \cdot \frac{x}{2,3 \cdot 10^3} = 19,99$$

$x = 1\ P(x,t) = 19,99$

$x = 10\ P(x,t) = 19,98$

$x = 100\ P(x,t) = 19,9$

$x = 1000 \, P(x,t) = 19,3$

For $v = \frac{100}{100 \cdot 10} = 0,1 \frac{<}{ACB} = 0,12 \cdot 10^{-5} < /A$

$$(20 - P) = 1,225 \cdot \frac{1,2 \cdot 10^{-3} 9,4 \cdot 10^2 \cdot 0,12 \cdot 10^{-5}}{0,4 \cdot 1,02 \cdot 10^{-12}} = 4,06 \cdot 10^6 = 4,06 \, 0$$

$$P(x,t) = 20 - 4,06 \frac{x}{l(t)}$$

$$x_1 = 1 P(x,t) = 19,99$$

$$x_1 = 10 P(x,t) = 19,98$$

$$x_1 = 100 P(x,t) = 19,8$$

$$x_1 = 1000 P(x,t) = 18,2.$$

Thus, the computational example allows for the assessment of the pressure distribution across the formation in discrete sections of the reservoir as the displacement front progresses. This, in turn, provides a timeline for the changes in the hydrodynamic pressure differential. It enables the determination of the duration and stages of pressure regulation during injection to achieve the expected hydrodynamic effect and, as a result, increase the oil influx to the production well gallery. This ensures a coordinated consideration of both the displacement conditions and the capacity-filtering characteristics of fluid-saturated reservoirs.

3 Pressure propagation in porous media

Here, particular interest lies in pressure waves in heterogeneous porous reservoirs, the main characteristics of which change significantly and non-linearly during the development process [25, 9]. Therefore, the process of mobilizing immobile zones is determined by the dynamics of pressure changes in the injected fluid.

The article further discusses the so-called "sharp regimes" [2], where one or more process characteristics grow unbounded over a finite time. For the process of hydrodynamically increasing pressure in the formation, sharp regimes should be introduced under the assumption of growth in pressure or injected fluid volume. In practice, these boundary characteristics are finite; however, as numerical calculations [2] have shown, the actual process of fluid entering the immobile pores under hydrodynamically increasing pressure can be considered as a sharp regime if the flow (or pressure) at the well increases several times compared to its initial value. Such an injection regime can be realized, for example, by a source with power that increases in steps. The work shows that under certain conditions, sharp regimes are more effective than conventional injection regimes.

A heterogeneous porous medium is considered as a system of two existing fictive continua, modeling systems of fractures and the porous blocks separated by them. The exchange of fluid between the fractures and blocks is caused by the difference in average pressures within them [4], with its modification [30], leading to the following filtration equations for weakly compressible droplet liquid:

$$\begin{cases} \frac{s \partial w_1}{\partial t} = \gamma_1 \nabla \left(w_1^3 \nabla w_1 \right) + \alpha \left(w_2 - w_1 \right) \\ \frac{\partial w_2}{\partial t} = \gamma_2 \nabla w_2 + \alpha \left(w_1 - w_2 \right), \quad w_i = p_i - \sigma \end{cases} \tag{3.1}$$

In equation (3.1), p_1 and p_2 represent the average pressures of the fluid in the fractures and blocks, respectively, $\gamma_1 w_1^3$ and γ_2 are the piezoconductivity coefficients, γ_2 is the pressure relaxation time, and ss is a coefficient defined in [30], which characterizes the physical properties of the medium.

Equations (3.1) are valid in the region where $p_1 > \sigma$; in the region where $p_1 < \sigma$, where filtration does not occur in the porous blocks, the usual equation for elastic filtration in blocks with a piezoconductivity coefficient γ_2 holds, which determines p_2 (or w_2). At the unknown boundary of the regions, the necessary conjugation conditions are satisfied [30].

In contrast to the equations proposed in [4], equation (2.1) accounts for the fact that the coefficient ss may be comparable to unity even in situations where the porosity in the immobile pores is much lower than the porosity in the mobile zones. Moreover, equation (2.1) takes into account the expansion (or contraction) of the immobile pores, leading to the dependence of the mobile fracture permeability on pressure. Both of these considerations are consistent with the experimental facts mentioned earlier (see also [23]).

In the case of gas filtration, instead of equation (3.1), the following equations can be obtained:

$$\begin{aligned} \frac{s\partial w_1^2}{\partial t} &= \gamma_1 \nabla \left(w_1^4 \nabla w_1 \right) + \alpha \left(w_2^2 - w_1^2 \right), \\ \frac{\partial w_2}{\partial t} &= \gamma_2 \nabla \left(w_2 \nabla w_2 \right) + \alpha \left(w_1^2 - w_2^2 \right), \end{aligned} \tag{3.2}$$

In processes of hydrodynamically increasing pressure in the formation, it is advisable to inject fluid at sufficiently high pressure ($p_1 \gg w_1$). In such conditions, the permeability of the mobile pores is typically much greater than the block permeability, and the capacity of the blocks is much smaller than the capacity of the mobile system (in both cases, the difference can reach several orders of magnitude). Therefore, at the initial stage of the process, it is acceptable to assume $w_1 - w_2 \approx w_1$. As a result, the first equations in (3.1) and (3.2) can be rewritten as follows:

$$\frac{\partial w}{\partial t} = D\nabla \left(w^{n-1} \nabla w \right) - \chi w, \; \chi = \frac{\alpha}{s}. \tag{3.3}$$

For the droplet liquid, $w_1 = p_1 - \sigma$, $n = 4$, $D = \gamma_1/s$, and for gas, $w = (p_1 - \sigma)^2$, $n = 5/2$, $D = \gamma_1/(2s)$.

In the future, for equation (3.3), we consider a one-dimensional problem with zero initial conditions in the region x>0x > 0, which corresponds to initially closed mobile pores. Using the variable substitution [3].

$$\begin{aligned} w &= u \, exp \left(-\chi t \right), \quad w = -\gamma \beta \left(\chi t \right) \\ \gamma &= D/ \left[n \left(n-1 \right) \chi \right], \quad \beta \left(t \right) = \exp \left[- \left(n-1 \right) \chi t \right] - 1 \end{aligned} \tag{3.4}$$

Instead of equation (3.3), we obtain

$$\partial u/\partial \omega = \partial \left(n u^{n-1} \, \partial u/\partial x \right) /\partial x, \quad u \left(-\infty, x \right) = 0 . \tag{3.5}$$

In accordance with the problem statement, let us consider the boundary condition (at $x = 0$, the flow $q \to \infty$ at $\omega \to -0$:

$$q \left(\omega, 0 \right) = q_0 \left(-\omega \right)^m, \quad -\infty < \omega < 0, \quad m \langle 0, \; q_0 \rangle 0 \tag{3.6}$$

(negative time is introduced for the self-similarity of the problem [8]).

The corresponding boundary condition (3.6) for the original problem also exhibits blow-up behavior:

$$\left(t, \; 0 \right) = q_0 \gamma^m \beta^m \left(t \right) \exp \left(-nxt \right) \tag{3.7}$$

By resolving the indeterminacy in (3.7) $t \to -\infty$, it can be shown that:

1 if $m < -n \left(n-1 \right)^{-1}$, the boundary and initial conditions are consistent (the injected fluid volume grows from zero).

2 if $m = -n \left(n-1 \right)^{-1}$, the injected volume instantaneously jumps from zero to $q_0 \gamma^m$ at the initial moment.

3 if $0 > m > -n(n-1)^{-1}$, the injected volume reaches maximum values.

The solution to the first boundary value problem can be obtained from the solution given below by substituting the coefficients [2].

Equation (3.5) with condition (3.6) has a self-similar solution [2, 18], from which, considering the transformation (3.4), we obtain the solution to the original problem (3.3).

$$w\left(t,x\right) = c\mu\left(t\right)\varphi\left(\xi\right), \quad x \leq x_* = \nu\left(t\right)\xi_*,$$

$$\mu\left(t\right) = \beta^{\frac{2m+1}{n+1}}\left(t\right)\exp\left(-\chi t\right), \quad \nu\left(t\right) = b\beta^{\frac{l}{n+1}}\left(t\right), \tag{3.8}$$

$$c = \left(n^{-1}q_0^2\gamma^{2m+1}\right)^{\frac{1}{n+1}}, \quad b = \left(nq_0^{n-1}\gamma^l\right)^{\frac{1}{n+1}}, \quad l = m\left(n-1\right)+n,$$

where x_* is the front of the wave opening immobile pores. The self-similar variable ξ is defined in terms of x and t similarly to (3.8).

The function $\varphi\left(\xi\right)$ in (3.8) is determined numerically (examples of calculations are shown in Fig. 1a) from an ordinary differential equation with boundary conditions:

$$\xi = 0, \quad \varphi^{n-1}d\varphi/d\xi = -1; \quad \xi \geq \xi_*, \quad \varphi = \varphi^{n-1}d\varphi/d\xi = 0$$

simultaneously with the coordinate $\xi_* = \xi_*\left(m,n\right)$ (Fig. 1b). All figures in the paper use dimensionless parameters.

Depending on the sign of the exponent l in (2.8), different regimes are possible [2]:

1. in the case $l < 0$ $w \to \infty$, $x_* \to \infty$ at $t \to -0$ (the fluid inflow exceeds its absorption by the blocks, and the zone of opened immobile pores increases indefinitely over time);
2. in the case $l = 0$, the zone of opened immobile pores is localized (fluid inflow and absorption are balanced), and the solution takes the form:

$$w = d\hat{\mu}\left(t\right)\left(1 - x/x_\alpha\right)^{\frac{2}{n-1}}, \tag{3.9}$$

$$x_\alpha = \left[2n\left(n+1\right)^n q_0^{n-1}/\left(n-1\right)\right]^{\frac{1}{n+1}}, \quad d = \gamma^{-\frac{1}{n-1}}\left[q_0^2\left(n^2-1\right)/\left(2n\right)\right]^{\frac{1}{n+1}},$$

where the symbol $\hat{\mu}\left(t\right)$ denotes the function $\mu\left(t\right)$ for $m = -n\left(n-1\right)^{-1}$.

In the case of $l > 0$, the second expression in (3.8) defines the effective half-width of the zone of opened fractures, which decreases over time (fluid absorption by the blocks exceeds its inflow).

Further, we will need the solution of (3.3) for the case of an instantaneous power source Q at the well, obtained in [3]:

$$w = \left[Q^2/\left(-\gamma\beta\left(t\right)\right)\right]^{\frac{1}{n+1}}\psi\left(\xi\right)exp\left(-\chi t\right), \quad \xi = x\left[-Q^{n-1}\gamma\beta\left(t\right)\right]^{-\frac{1}{n+1}},$$

$$\psi\left(\xi\right) = \begin{cases} C\left[1 - \left(\xi/\xi_0\right)^2\right]^{\frac{1}{n-1}}, & 0 \leq \xi \leq \xi_0, \\ 0, & \xi \geq \xi_0, \end{cases} \tag{3.10}$$

where the constants ξ_0 and C are determined by the parameter n (for $n=3.5$n = 3.5, $\xi_0 \approx 1,87$, $C \approx 1,26$).

The effect of fluid absorption by the blocks results in the front of the opening of immobile pores tending, as follows from (3.10) and (3.4), to the limiting position x_0 as $t \to \infty$:

$$x_0^{n+1} = \xi_0^{n+1}Q^{n-1}D/\left[n\left(n-1\right)\chi\right] \tag{3.11}$$

In the absence of absorption, the front moves indefinitely away from the well over time.

Let us determine the efficiency of applying blow-up regimes in hydraulic fracturing compared to impulse fluid injection (solution (3.10)). For blow-up regimes, the total fluid flow at the well is given by

$$Q = q_0 \int\limits_{-\infty}^{\omega} (-\omega)^m \, d\omega = -\frac{q_0}{m+1} (-\omega)^{m+1} \tag{3.12}$$

Eliminating time ω from (3.12) and the expression for the self-similar variable ξ in (3.8), we obtain the front of fracture opening as a function of the parameters $Q, \ m$:

$$x_*^{n+1} = n\xi_*^{n+1} \left[(-m-1)^l \, Q^l / q_0 \right]^{\frac{1}{m+1}} \tag{3.13}$$

Using (3.11) and (3.13), we form the ratio

$$x_*/x_0 = A(m)\, \eta, \tag{3.14}$$

where

$$A(m) = (\xi_*/\xi_0) \left[n(-m-1)^{\frac{l}{m+1}} \right]^{\frac{1}{n+1}}, \ \eta = \left[\gamma^{-1} (Q/q_0)^{\frac{1}{m+1}} \right]^{\frac{1}{n+1}}.$$

Let $l < 0$. The coefficient $l < 0$ in (3.14) monotonically increases with increasing m. For $n = 3, 5$, the calculated dependence $A = A(m)$ turned out to be quite close to the dependence $\xi_* = \xi_*(m)$. The parameter η in (3.14) also depends on m; however, this dependence can be compensated by an appropriate selection of $q_0 = q_0(m)$ since, for $l < 0$, the flow at the well increases from zero at the initial moment, and the coefficient q_0 in (3.6) is arbitrary.

With such a selection, the dependence (3.14) is linear. The lines located above the bisector $(-1, 4 = -n/(n-1) > m \gtrsim -1, 72)$ correspond to a larger fracture zone obtained in the blow-up regime for $l < 0$ compared to the impulse action of the source [9].

Let us clarify the obtained results. For $l > 0$, the initial flow rate at the boundary is sufficiently high, and the subsequent increase in flow is weak (small values of $|m|$ in (3.7), $0 > m > -n/(n-1), 0 > m > -n/(n-1)$. When the total volume of fluid for hydraulic fracturing, Q, is specified, this volume will be used up fairly quickly in this case (in the limit, at the initial moment in time), and the further advancement of the immobile pore opening front will not be "supported" (in contrast to fluid absorption by the blocks) by an increase in the boundary flow rate. Absorption leads to a reduction in the effective zone of immobile pore opening fractures, which was initially created by the impulse injection.

For $l < 0$, the boundary flow rate grows from zero at a fast pace (large values of $|m|, m < -n/(n-1)$), and the advancement of the immobile pore opening front is "supported" by the increasing flow at $x = 0$. However, the increase in boundary flow rate should be moderato $|m|$ is too large, the given fluid flow will be quickly consumed, and the advancement of the immobile pore opening front will cease. The largest fractured zone is obtained at the optimal balance between fluid injection and absorption processes, which occurs, when $l = 0 \ m = -n/(n-1)$. In this case, the front moves more slowly than for $l < 0$. The size of the fractured zone (3.9) depends on the system's nonlinearity parameter n and q_0 [22, 25].

Now, let us examine the effect of absorption on the process of hydrodynamic pressure increase during hydraulic fracturing for $l = 0$. Assume that the parameters D and n in (3.3) are fixed. Consider two types of blocks with absorption coefficients $\chi_1 < \chi_2$, and therefore, according to (3.4), $\gamma_1 > \gamma_2$.

For $l = 0$, the injected fluid flow increases abruptly at the initial moment from zero to the value $\hat{q}_0 = q_0/\gamma^{|m|}, \ m = -n/(n-1)$. For given values of $\hat{q}_0, Q$, we find $q_{02} =$

$q_{01} (\gamma_2/\gamma_1)^{|m|}$, and using (3.9), we obtain the relationship between the sizes of the immobile pore fractured zones:

$$(x_{\alpha_2}/x_{\alpha_1})^{n+1} = (\chi_1/\chi_2)^{|m|} < 1.$$

Thus, for a given total fluid flow, a smaller fractured zone will be created in a medium with higher absorption. For example, if $(\chi_2/\chi_1) = 2$ and $n = 3, 5$, we find $(\chi_{\alpha_2}/\chi_{\alpha_1} \approx 0, 12)$.

Now, let us assume that the size of the created immobile pore fractured zone is specified. Using (3.11) and (3.13), we form the ratio of the fluid flow Q under impulse source action to the flow Q_* in the blow-up regime for $l < 0$:

$$Q/Q_* = B(m)\eta, \tag{3.15}$$

where

$$B = \left[n(-m-1)^{\frac{l}{m+1}} (\xi_*/\xi_0)^{n+1} \right]^{\frac{1}{n-1}}, \ \eta = \left[\gamma^{-1} (Q_*/q_0)^{\frac{1}{m+1}} \right]^{\frac{1}{n-1}}.$$

Field Studies

Laboratory studies served as the basis for the field implementation of a technological solution aimed at influencing a heterogeneous reservoir with residual, stagnant oil-saturated zones [36 – 38]. The method was applied during a technological operation on a group of wells at the offshore Bohai Bay field, operated by the CNOOC oil company (China).

Operation was conducted in a section of the reservoir that included 14 production wells responding to water injection. The technology was implemented with the support of *New Horizon Company* at the injection well C12. Field operation, carried out through displacement, consisted of several sequential stages of hydrodynamic impact by implementing cycles of increasing and decreasing injection pressure (Fig. 5).
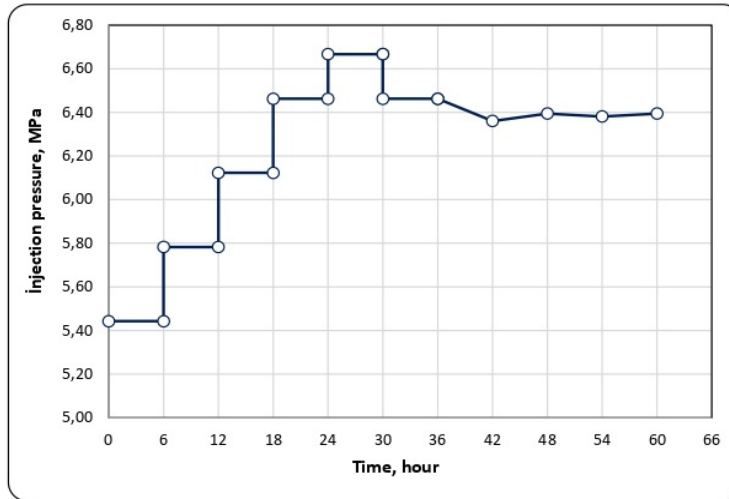

Fig. 5. Dynamics of pressure changes during the hydrodynamic impact on injection well C12 (Penglai field, CNOOC)

At the end of the field operation, monitoring of injection pressure indicators and water injection volume at the injection well was carried out (Figure 6).
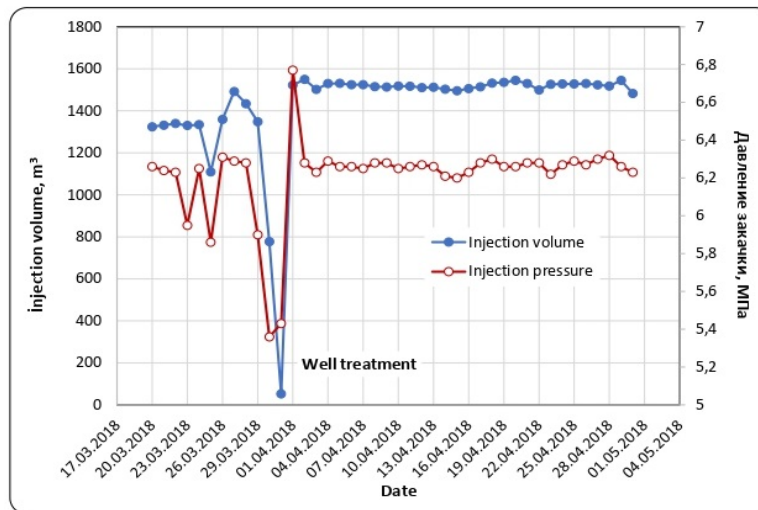
Fig. 6. Changes in the current performance indicators of injection well C12

As the monitoring of the main operational indicators of the surrounding (reacting) wells in the area of technology implementation showed, in general, all wells have a positive reaction to the hydrodynamic impact - the majority of production facilities have an increase or stabilization of the values of average daily oil flow rate. Fig. 7 shows the actual dynamics of oil flow rate and water cut after the implementation of technological operation at well C54ST2 of Penglai field.
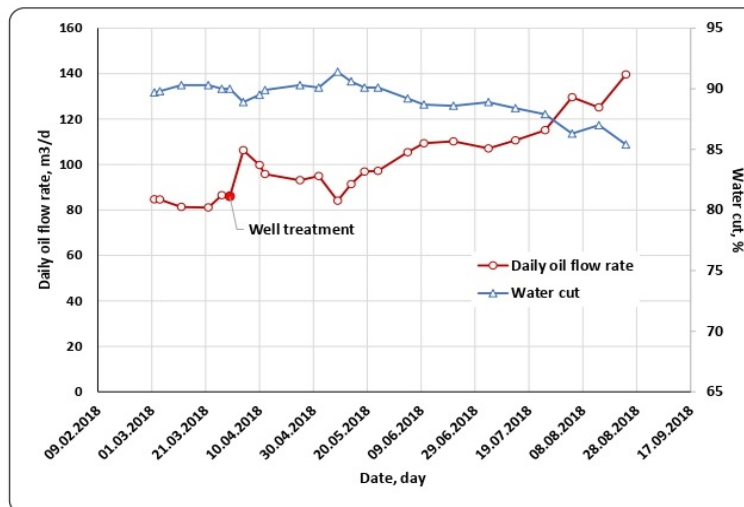
Fig. 7. Trends of average daily oil flow rate and water cut at the reacting well of the technology implementation site

4 Conclusions

Laboratory studies have shown that capillary processes and instability of the front of oil displacement by water are important elements of the dependence of residual oil saturation on hydrodynamic pressure in the reservoir. It should be taken into account that the intensity and direction of capillary forces depend on numerous physical and physical-chemical properties

of reservoir systems, rocks, reservoir fluids, including displacement conditions. One of the ways to optimize the impact on the deposit taking into account capillary processes occurring in the reservoir system is to create a consistent periodically increasing hydrodynamic pressure.

References

1. Abou-Sayed, A.S., Zaki, K.S., Wang, G., Sarfare, M.D., Harris, M.H. (2007) Produced Water Management Strategy and Water Injection Best Practices, Design, Performance, and Monitoring, SPE Production & Operations 22, 1, p. 59 – 68.

2. Barenblatt, G.I., Entov, V.M. & Ryzhik, V.M. (1990). Theory of Fluid Flows Through Natural Rocks. Kluwer Academic Publishers, Dordrecht, Boston, London.

3. Buevich, Y.A. On the theory of joint filtration of immiscible fluids in a gravity field. Fluid Dyn 2, 113–114 (1967). https://doi.org/10.1007/BF01015158

4. Buevich, Y.A., Mambetov, U.M. Toward a theory of the simultaneous filtration of immiscible liquids. Journal of Engineering Physics 60, 84–91 (1991). https://doi.org/10.1007/BF00871618.

5. Chacon, Abel & Tiab, Djebbar. (2007). Effects of Stress on Fracture Properties of Naturally Fractured Reservoirs. 10.2118/107418-MS.

6. Dimov S.V. Dvumernoe modelirovanie obrazovaniya ostatochnoj nasyshchennosti odnoj iz faz pri fil'tracii nesmeshivayushchihsya zhidkostej // Izv. SO AN - Ser. tekh. nauk 1988. - N6. - p. 93-96.

7. Dimov S.V. Vytesnenie gangliev nesmachivayushchej zhidkosti iz poristoj sredy // Sb. Aktual'nye voprosy teplofiziki i fizicheskoj gidrodinamiki. - Novosibirsk. - 1988. – p. 165 - 172.

8. Dimov S.V., Kuznecov V.V. Usloviya mobilizacii nesmachivayushchej fazy v poristoj srede // Izv. AN SSSR MKT. - 1988. - no 6. - p. 104 - 111.

9. Entov V.M., Mirzadzhanzade A.H., Mishchevich V.I. // PMTF. 1971. no 4.

10. Entov V.M., Zazovskij A.F. Gidrodinamika processov povysheniya nefteotdachi. - M.: Nedra, 1989. - 232 p.

11. Gimatudinov SH.K. Fizika neftyanogo i gazovogo plasta. - M.: Nedra, 1971, 310 p.

12. Gorbunov A.T., Buchenkov L.N. Shchelochnoe zavodnenie. – M: Nedra, 1989. – 160 p.

13. Gubanov B.F. Regulirovanie profiley priemistosti nagnetatel'nyh skvazhin // Neftyanoe hozyajstvo, no.12, 1981. – p. 39 - 42.

14. Habibulin M.YA. Eksperimental'no-teoreticheskie issledovaniya vytesneniya nefti vodoj, s ciklicheski izmenyayushchejsya amplitudoj davleniya // Elektronnyj nauchnyj zhurnal "Neftegazovoe delo", 2012, ¹ 6. – S. 233 - 241.

15. Hanzlik E.J. and MimsI D.S. Forty Years of Steam Injection in California-The Evolution of Heat Management // 2003 SPE International Improved Oil Recovery Conference, Kuala Lumpur, 20-21 October.

16. Harin O.N. Vyvod raschetnyh formul dlya priblizhennoj ocenki effektivnosti ciklicheskogo vozdejstviya na plast. – Trudy INGP im. I.M. Gubkina. Teoriya i praktika razrabotki neftyanyh mestorozhdenij. - M.: Nedra. – 1967. – p. 122 – 130.

17. Harwell M.A., Gentile H. Ecological Significance of Residual Exposures and Effects Oil Spill. – M.: InTech, 2006. – 246 p.

18. Ishii, K.; Pierre, M.; Suzuki, T. Quasilinear Parabolic Equations Associated with Semilinear Parabolic Equations. Mathematics 2023, 11, 758. https://doi.org/10.3390/math11030758.

19. Islam, M.R. Cosurfactant-Enhanced Alkaline/Polymer Floods for Improving Recovery in a Fractured Sandstone Reservoirs // Particle Technology and Surface Phenomena in

Minerals and Petroleum, eds. Sharma and Sharma, Plenum Publishers, NY, 1991, pp. 223-233.

20. Khasanov M.M., Ushmaev O., Nekhaev S., Karamutdinova D., The optimal parameters for oil field development (In Russ.), SPE-162089-MS, 2012, DOI: https://doi.org/10.2118/201987-MS.

21. Larson R.J., Davis H.T., Scriven L.E. Chem. Eng. Sci, 1981, v. 36, N 1, p 75-85.

22. Liu, Huaxun & Gao, Shusheng & Ye, Liyou & Zhu, Wenqing & An, Weiguo. (2021). Change laws of water invasion performance in fractured–porous water-bearing gas reservoirs and key parameter calculation methods. Natural Gas Industry B. 8. 10.1016/j.ngib.2020.06.003.

23. Martinson, L & Pozdyshev, M & Andreev, A. (2019). Spatial localization of thermal structures. Journal of Physics: Conference Series. 1348. 012102. 10.1088/1742-6596/1348/1/012102.

24. Mihaylov N.N., Kol'chickaya T.I., Dzhemesyuk A.V., Semenova N.A. Fiziko-geologicheskie problemy ostatochnoj neftenasyshchennosti. - M.: Nauka, 1993 – 173 p.

25. Mirzadzhanzade A.H., Ogibalov P.M. Mekhanika fizicheskih processov. M., izd. MGU, 1980.

26. Mirzadzhanzade A.H., Shahverdiev A.H. Dinamicheskie processy v neftegazodobyche. - M.: Nauka, 1997 g. – 254 p.

27. Musyaev R.A., Dzhafarli S.Z., Halilov E.G., Gashimov A.F. O vozmozhnosti povysheniya effektivnosti shchelochnogo zavodneniya plastov, soderzhashchih neaktivnye nefti // Trudy instituta problem glubinnyh neftegazovyh mestorozhdenij. // " Nafta-Press", Baku. – 1999. – 178 p.

28. Nakoryakov V.E., Kuznetsov V.V. Teplomassobmen i volnovye processy pri dvuhfaznom techenii v poristyh sistemah i zasypkah // Prikladnaya mekhanika i tekhnicheskaya fizika, 1997, t. 38, no.4, p. 155 – 166.

29. Nefti SSSR, Spravochnik, M.: Himiya, t. 1, 1974, 504 p.

30. Nigmatulin, R.I., Gubaidullin, A.A. (1991). Fundamentals Of Mechanics Of Saturated Porous Media: Basic Equations And Waves. In: Kakaç, S., Kilki, B., Kulacki, F.A., Arinch, F. (eds) Convective Heat and Mass Transfer in Porous Media. NATO ASI Series, vol 196. Springer, Dordrecht. https://doi.org/10.1007/978-94-011-3220-6.

31. Richardson, et al. Chemically assisted thermal flood process United States Patent 6,305,472. October 23, 2001.

32. Roland Lenormand, Eric Touboul and Cesar Zarcone Numerical models and experiments on immiscible displacements in porous media // Journal of Fluid Mechanics / Volume 189 / April 1988, pp 165 no 187.

33. Rybak B.M. Analiz nefti i nefteproduktov. Izd. 5-e pererab. i dop. -M.: Gostoptekhizdat, 1962. - 888 p.

34. Saffman P.G., Taylor G.I. Proc.Roy.Soc. London A 245, 312 (1958).

35. Schulz H. E. Hydrodynamics – Optimizing Methods and Tools. – M.: InTech, 2011. – 420 p.

36. Sergiyenko S.R. Vysokomolekulyarnye soedineniya nefti. M.: Himiya, 1964, 542 s.

37. Shahverdiev A.H., Panahov G.M., Abbasov E.M. Sinergeticheskie effekty pri sistemnom vozdejstvii na zalezh' termo-reohimicheskimi tekhnologiyami // Neftyanoe hozyajstvo, M.: no. 11. – 2002. p. 61-65.

38. Shelkachev V.H. Obobshchenie formy reshenij prostejshih osnovnyh zadach teorii nestacionarnogo polya filtracionnyh potokov – Trudy INGP im. I.M. Gubkina. Teoriya i praktika razrabotki neftyanyh mestorozhdenij. - M.: Nedra. – 1967. – p. 96 – 106.

39. Snow N., Tippee B. Journal Optimizing Methods of Exploitation Oil Field // Oil&Gas. – 2013. – no. 21. – P. 18–21.

40. Snow N., Tippee B. Journal Optimizing Methods of Exploitation Oil Field // Oil& Gas. – 2013. – no 21. – P. 18–21.
41. Surguchev M.L. Vtorichnye i tretichnye metody uvelicheniya nefteotdachi. – M.: Nedra, 1985. – 308 p.
42. Surguchev M.L., ZHeltov YU.V., Simkin E.M. Fiziko-himicheskie mikroprocessy v neftegazonosnyh plastah: Nedra, 1984. – 215 p.
43. Tayfun Babadagli Evaluation of EOR methods for heavy-oil recovery in naturally fractured reservoirs // Journal of Petroleum Science and Engineering, 37 (2003) 25-37.
44. Taylor, K.C., Hawkins, B.F. and Islam, M.R., 1990, Dynamic Interfacial Tension in Surfactant-Enhanced Alkaline Flooding, J. Canadian Petroleum Technology, vol. 29 (1), 50-55.
45. Xing, Cuiqiao & Yin, Hongjun & Liu, Kexin & Li, Xingke & Fu, Jing. (2018). Well Test Analysis for Fractured and Vuggy Carbonate Reservoirs of Well Drilling in Large Scale Cave. Energies. 11. 80. 10.3390/en11010080.
46. Yemaletdinov A.K., Bajkov I.V. Modelirovanie optimal'noj skorosti vytesneniya nefti i minimal'noj neftenasyshchennosti vokrug nagnetatel'nyh skvazhin // Vestnik Orenburgskogo Gosudarstvennogo Universiteta, no2. – 2005. – p. 159 – 162.
47. Yershov A.P., Dammer A.YA., Kupershtoh A.L. Neustojchivost "nevyazkogo palca" v regulyarnyh modelyah poristoj sredy // Prikladnaya Mekhanikai Tekhnicheskaya fizika, 2001, t. 42, no 2. – p. 129-140.
48. Yevdokimova V.A., Kochina I.N. Sbornik zadach po podzemnoj gidravlike. - M.: Nedra, 1979. - 168 p.
49. Zheltov YU.N. Mekhanika neftegazonosnogo plasta. M.: Nedra, 1975. – 216 p.